

## Structural Investigation of Poly( $\gamma$ -benzyl-L-glutamate) (DP1100)

Sujata RATH

Lecturer in Physics, S.G. Women's College, Rourkela-769006, India

(Received March 11, 1998)

**ABSTRACT:** Small-angle X-ray scattering (SAXS) technique has been used to investigate various macromolecular structural parameters of poly( $\gamma$ -benzyl-L-glutamate) (PBLG) with degree of polymerization (DP) 1100. The SAXS profile of the sample deviates from Porod's law establishing that it falls under non-ideal two-phase structure characterized by continuous variation of electron density at the phase boundary. The theories developed by Vonk (1973) and Ruland (1971) for non-ideal two-phase structures have been applied to calculate different parameters such as  $D$ , the transverse periodicity,  $\phi_1$  and  $\phi_2$  the volume fractions of matter and void phases respectively,  $T_1$  and  $T_2$ , transversal lengths,  $\bar{l}_r$  range of inhomogeneity, and  $\bar{l}_c$ , length of coherence. The two values of  $E$ , width of transition layer, have been obtained by the method of Vonk and Ruland.

**KEY WORDS** Non-Ideal Two-Phase System / Enhancement of Scattering / Corrugation of the Surface / Polypeptide Poly( $\gamma$ -benzyl-L-glutamate) / One- and Three-Dimensional Correlation Functions / Constant Background Intensity /

In practice, Porod's law<sup>1,2</sup> is best obeyed in polymers with a high crystallinity. Polymers of lower crystallinity often show more rapid decrease of the intensities in the tail of the diffraction curve than predicted by Porod's law, indicating the presence of transition layer. By applying Porod's law, to the background corrected intensity,  $\tilde{I}(q) \cdot q^3$  does not reach a constant value at large  $q$  causing enhancement of scattering at high angle, leading to positive slope of  $\tilde{I}(q) \cdot q^3$  versus  $q^2$  which occurs when electron density instead of remaining constant within phases may have long range fluctuation from the mean value in either or both phases. This is known as positive deviation from Porod's law. The existence of diffuse phase boundary causes a depletion of high angle scattering leading to a negative slope for a similar plot. This is referred to as negative deviation from Porod's law.<sup>3,4</sup> In our piece of work, the later type of distortion only is observed due to corrugation of the surface of the particle (Vonk<sup>5</sup>) giving rise to large surface area. This results in the absence of weak boundaries enhancing fracture toughness.

According to Ruland<sup>6</sup> for many systems, the phase boundary may not be sharp but characterized by certain range  $E$ , known as width of transition layer. Later Vonk<sup>5</sup> has developed practical aspects of Ruland method and such methods are referred to as non-ideal two-phase systems.

Iizuka<sup>7</sup> has pointed out that electrically and magnetically oriented films of polypeptide poly( $\gamma$ -benzyl-L-glutamate) (PBLG) have a lamellar texture ranging from a few to several micrometers in thickness with lamellae perpendicular to the external field direction. The gap regions between two adjacent lamellae have been detected by Iizuka<sup>7</sup> and these observations appear strong indications of the presence of molecular clusters. Sobajima<sup>8</sup> has pointed out that the orientation of PBLG in isotropic state becomes observable in a magnetic field. This property of PBLG enables it to be conveniently handled for fine structure investigation by small-angle scattering method.

These studies will be of great importance in the field of Biophysics. Stewart<sup>9</sup> made a novel statement about

the role of liquid crystals in living systems. These are the ideal building blocks for living systems. Therefore small-angle X-ray scattering (SAXS) study of the sample throws more light on the macromolecular structural aspect of the system.

### X-RAY MEASUREMENT

SAXS measurements were made at the Centre of Advanced studies (Physics), University Department of Chemical Technology, Matunga, Bombay, by a compact Kratky camera.<sup>10</sup> The entrance slit and counter slit attached to the camera were adjusted at 80  $\mu\text{m}$  and 120  $\mu\text{m}$ , respectively. X-Ray radiation was obtained from a Philips generator with a copper target operated at 40 kV and 20 mA and the monochromatization was achieved using a Nickel filter of 10  $\mu\text{m}$  thickness. The monochromatic Cu- $K_\alpha$  ( $\lambda = 1.54 \text{ \AA}$ ) radiation thus obtained is used to irradiate the samples by inserting them in mark capillary tubes of 1 mm diameter. To reduce the scattering of X-rays by air between the sample and detector, vacuum in the intervening space was maintained at a pressure of about 1/2 mbar. The distance of the sample to the detector ' $a$ ' was kept at 20 cm.

### THEORY

When absolute intensity is not available, a very useful parameter  $R^{11}$  for the characterization of structure is given by

$$R = \frac{\langle |\text{grad } \eta|^2 \rangle}{\langle \eta^2 \rangle} = 6\pi^2 \frac{\int_0^\infty s^3 \tilde{I}(s) ds}{\int_0^\infty s \tilde{I}(s) ds} \quad (1)$$

where  $s$  is the coordinate in the reciprocal or Fourier space given by  $s = 2\theta/\lambda$  where  $2\theta$  is the scattering angle and equal to  $\lambda q/2\pi$ , where  $q$  is given by the relation

$$q = \frac{4\pi \sin \theta}{\lambda} = \frac{4\pi\theta}{\lambda}, \quad \theta \rightarrow 0$$

This equation is in agreement with Porod's law in the sense that in the presence of an infinitely sharp phase boundary the gradient at the phase boundary will become infinite, whereas at the same time because of Porod's law, the integrals in the numerator at the right hand side will no longer converge.

In an ideal two-phase structure, the gradient at the phase boundary is infinite and consequently  $R$  goes to infinity. In a two-phase structure showing diffuse phase boundary, the gradient of the electron density will have a value different from zero only inside the transition region of width  $E$ . So the value of  $R$  determines the nature of the sample as to whether it belongs to an ideal or non-ideal two-phase system. This relation (1) when changed to variable  $q$  gives,

$$R = 3/2 \frac{\int_0^\infty q^3 \tilde{I}(q) dq}{\int_0^\infty q \tilde{I}(q) dq} \quad (2)$$

According to Vonk, the relation

$$\langle |\text{grad } \eta|^2 \rangle = \Delta\eta^2 S/E_v V \quad (3)$$

holds good for a pseudo two-phase structure, where  $E_v$  is the width of transition layer after Vonk;  $\Delta\eta = \eta_1 - \eta_2$ , is the electron density difference of the two phases,  $\eta$ , is the deviation of electron density from the mean value and  $S/V$ , is the specific inner surface of the phase boundary per unit volume of dispersed phase.

According to Debye *et al.*,<sup>12</sup>  $S/V$ , for a pseudo two-phase structure can be found from the slope of the three-dimensional correlation function at the origin given by,

$$\left[ \frac{dC(r)}{dr} \right]_{r=0} = \frac{-S}{4V} \frac{\Delta\eta^2}{\langle \eta^2 \rangle} \quad (4)$$

Here, in view of the curvature of the correlation function near the origin, the slope has to be found at a distance where it is constant, which is at least at distance  $E$  from the origin. Combining relations (1), (3), and (4)

$$E_v = -\frac{4}{R} \left[ \frac{dC(r)}{dr} \right]_{r=E_v} \quad (5)$$

To calculate  $E_v$ , one has to evaluate  $C(r)$ , the three-dimensional correlation function at various of  $r$  in real space. Mering and Tchoubar<sup>13</sup> showed that  $C(r)$  can be calculated from the expression,

$$C(r) = \int_0^\infty s \tilde{I}(s) \cdot J_0(2\pi rs) ds / \int_0^\infty s \tilde{I}(s) ds \quad (6)$$

where  $z = qy$  and  $J_0$  is the Bessel function of zero order of the first kind. This eq 6 can be written in terms of  $q$  as,

$$C(r) = \int_0^\infty q \tilde{I}(q) J_0(rq) dq / \int_0^\infty q \tilde{I}(q) dq \quad (7)$$

Again the one-dimensional correlation function  $C_1(Y)$  for a lamellar system by Mering and Tchoubar<sup>13</sup> when changed to  $q$  variable reduces to,

$$C_1(y) = \frac{\int_0^\infty q \tilde{I}(q) [J_0(z) - zJ_1(z)] dq}{\int_0^\infty q \tilde{I}(q) dq} \quad (8)$$

Here  $J_1$  is the Bessel function of the first order of first kind. Vonk<sup>5</sup> has shown that the position of the first subsidiary maximum in one-dimensional correlation function gives  $D$ , the average periodicity transverse to the layer. The relation,

$$\left[ \frac{dC_1(y)}{dy} \right]_{y>E} = -\frac{1}{D} \frac{\Delta\eta^2}{\langle \eta^2 \rangle} \quad (9)$$

derived by Vonk<sup>5</sup> can be used to calculate  $\Delta\eta^2/\langle \eta^2 \rangle$ . Here the slope is taken at a point where  $y$  is greater than  $E$ .

The derivatives of three- and one-dimensional correlation function at the origin can be shown to be related to each other by Vonk<sup>5</sup>

$$\left[ \frac{d^2 C_1(y)}{dy^2} \right]_{y=0} = 3 \left[ \frac{d^2 C(r)}{dr^2} \right]_{r=0} \quad (10)$$

The presence of a transition region also affects the correlation function. For a pseudo two-phase structure, this function shows a discontinuity in the second derivative. But this is removed by the presence of a transition layer, in which case the following relation holds.<sup>14</sup>

$$\left[ \frac{d^2 C(r)}{dr^2} \right]_{r=0} = -\frac{R}{3} \quad (11)$$

For a layer structure, as shown by Vonk,<sup>5</sup>  $S/V$ , can be written as

$$S/V = 2/D \quad (12)$$

For a non-ideal two-phase structure, the following relation holds good Vonk<sup>5</sup>

$$\left[ \frac{\langle \eta^2 \rangle}{\langle \Delta\eta^2 \rangle} \right] = \left[ \phi_1 \phi_2 - \frac{S}{V} \cdot \frac{E}{6} \right] \quad (13)$$

where  $\phi_1$  and  $\phi_2$  are the volume fractions of the two-phases, *i.e.*, matter and void phase, respectively. Assuming the sum of the above volume fractions to be unity,  $\phi_1$  and  $\phi_2$  can be determined from relation (13).

According to Mittelbach and Porod<sup>15</sup> and Porod,<sup>2</sup>  $\bar{l}_1$ , the average length in matter region and  $\bar{l}_2$ , the average length in void region are given by

$$\bar{l}_1 = 4\phi_1 V/6 \quad (14)$$

and

$$\bar{l}_2 = 4\phi_2 V/S \quad (15)$$

with the range of inhomogeneity,  $\bar{l}_r$ , as

$$\frac{1}{\bar{l}_r} = \frac{1}{\bar{l}_1} + \frac{1}{\bar{l}_2} \quad (16)$$

The length of coherence,  $\bar{l}_c$ , as given by the above workers is,

$$I_c = 2 \int_0^\infty C(r) dr \quad (17)$$

The method for estimating  $E$  has been given by Ruland.<sup>16</sup> The functional relation of  $\tilde{I}(s)$  with  $s$  at the tail end of the SAXS pattern, for non-ideal two-phase system is given by

$$\tilde{I}(s \rightarrow \infty) = \frac{\pi c}{2} \left[ \frac{1}{s^3} - 2\pi^2 \frac{E^2}{3s} \right] \quad (18)$$

where  $C$  is a proportionality constant. For an ideal two-phase system,  $E=0$  and hence the above equation reduces to Porod's law. When transformed to  $q$  variable,

$$\tilde{I}\langle q \rightarrow \infty \rangle \cdot q = 4\pi^4 c \cdot q^{-2} - 4\pi^4 c E^2 / 6 \quad (19)$$

$E_R$  can be obtained from the graph of  $\tilde{I}(q) \cdot q$  versus  $q^{-2}$  commonly known as Ruland plot.

### BACKGROUND CORRECTION

Apart from density variation resulting from the presence of different phases, most samples show density fluctuations in liquids due to thermal motion. In polymers, such motion may be frozen at the temperature of observation, but this in principle makes no difference to the X-ray diffraction curve.<sup>17</sup> The resulting density variation can be shown<sup>18</sup> to give rise to a background, which in the  $2\theta$  region of SAXS of most polymers is constant or increases slightly with diffraction angle. In case of small-angle scattering this background can be considered wide-angle scattering extending into the small-angle region. In cases where a constant background level over a sufficient large  $2\theta$  interval between the SAXS and amorphous halo can be observed, this level may be simply subtracted from the total observed intensity.

If no such region of constant intensity is present, or if data of very high quality are desired, one may resort

to more elaborate methods for assessing the shape of the background curve. These may involve melting of the sample, as described by Korteleva *et al.*<sup>19</sup> Also one may apply an empirical procedure for extrapolating the observed non-constant background  $\tilde{I}_{bg}$  to smaller angles. To this end, equations of the type

$$\tilde{I}_{bg} = ae^{-b(2\theta)^2}$$

and

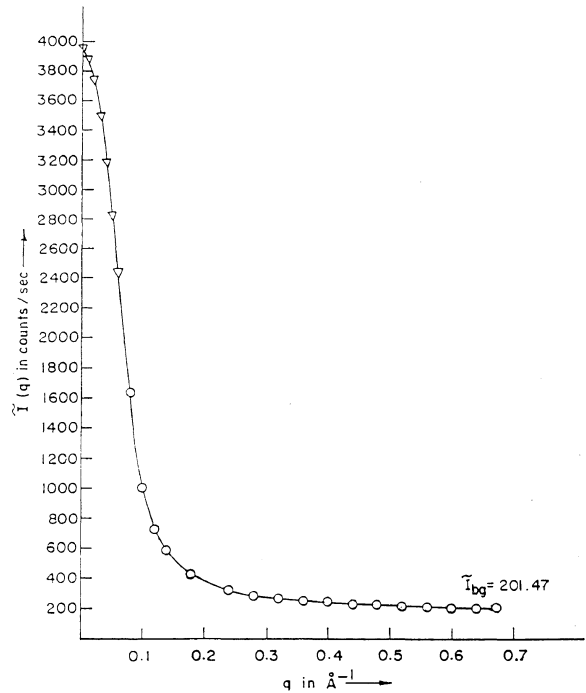


Figure 1. Smear-out scattering plots of PBLG (DP 1100); extrapolated points appear as reverse triangles.

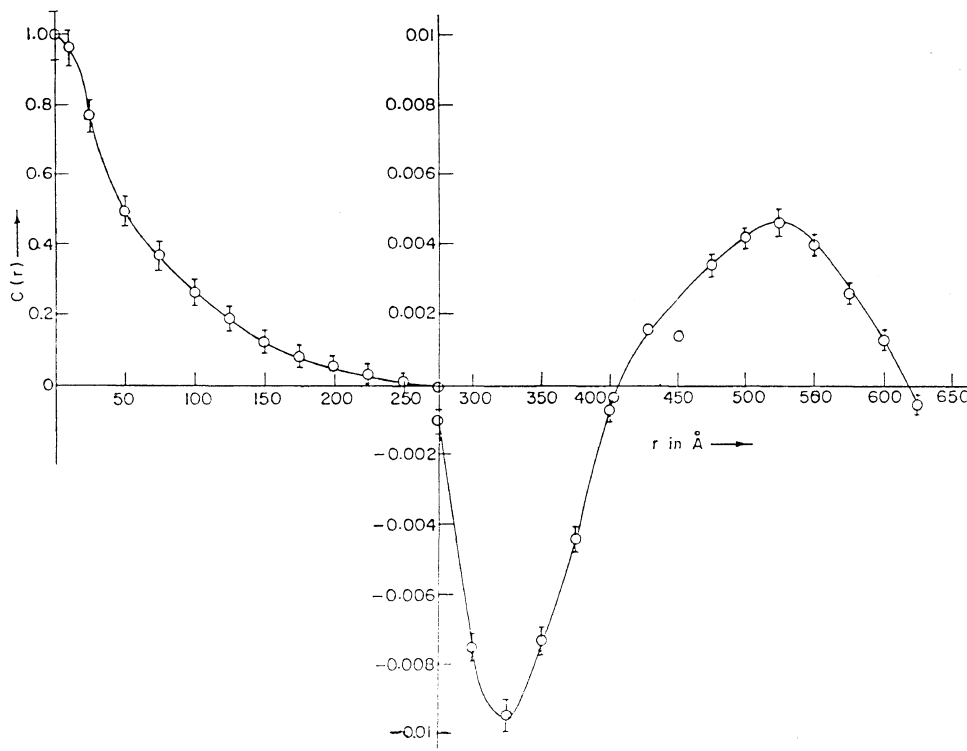


Figure 2. Curve of three-dimensional correlation function  $C(r)$  plotted against  $r$  with error bars.

$$\tilde{I}_{bg} = a + b(2\theta)^n$$

have been proven to be useful.<sup>20,5</sup> Here  $a$  and  $b$  are constants and  $n$  is an even number giving the best fit to the data points in the chosen interval between SAXS and wide-angle X-ray scattering (WAXS).

Since the correlation function at the origin is very sensitive to error in the tail end of the scattering curve (Vonk<sup>5</sup>), it is absolutely necessary to find the background scattering for the whole observed range.

For the above assumptions corresponding to background intensity,  $E$ , the width of transition layer, when calculated following the methods of Vonk and Ruland shows only a relatively small difference. So one is justified in deducting a constant background intensity corresponding to a minimum intensity value in the SAXS pattern<sup>11</sup> as in our case. These background corrected intensities have been used in subsequent analysis, with 5% statistical error in intensity data as observed by our experimental study. The effect of this error has been taken care of in subsequent calculations of correlation functions and error bars have been plotted. At appropriate places, the limits of error resulting from the intensity fluctuation have been incorporated while evaluating the various parameters. In our work, constant background intensities marked as  $\tilde{I}_{bg}$  in Figure 1 is deducted.

#### APPLICATIONS AND RESULTS

Five intensity values near the origin were fitted to the Gauss curve (Vonk<sup>21</sup>)

$$\tilde{I}(q \rightarrow 0) = P \cdot \exp(-Qq^2)$$

by least square technique and constant  $P$  and  $Q$  were 3949.41 and 134.41, respectively. Taking these values of  $P$  and  $Q$ , the scattering curve for the sample was extrapolated and is shown in Figure 1. The extrapolation has very little effect on the relevant part of the correlation functions. Neither the position nor the height of the first

subsidiary maximum of the one-dimensional correlation function is much affected.<sup>11</sup>

Using relation (7) the three-dimensional correlation function  $C(r)$  was computed for various values of  $r$  and is shown in Figure 2, with error bars. As per eq 11 the value of

$$-3 \left[ \frac{d^2 C(r)}{dr^2} \right]_{r=0} \text{ is } 2.772 \times 10^{-3} \text{ \AA}^{-2}$$

which is in good agreement with  $R$  indicating that the sample is isotropic. The slope of  $C(r)$  at different points was computed by numerical differentiation applying five point central difference formula with a regular interval of 1  $\text{\AA}$ .  $[-(4/R) \cdot (dC(r)/dr)]$  versus  $r$  for each sample is plotted in Figure 3. The value referred to as  $E_v$ , is also shown in the figure.

Since PBLG has a layer structure,<sup>7</sup> the one-dimensional correlation function  $C_1(y)$  applicable for layer structure was calculated for the sample using relation (8) for various values of  $y$ .

$G_1(y)$  versus  $y$  with error bars is shown in Figure 4.

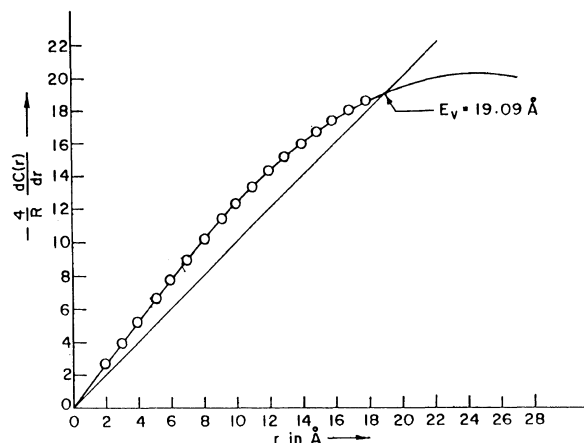


Figure 3. Curve of  $-(4/R)[dC(r)/dr]$  plotted against  $r$ .

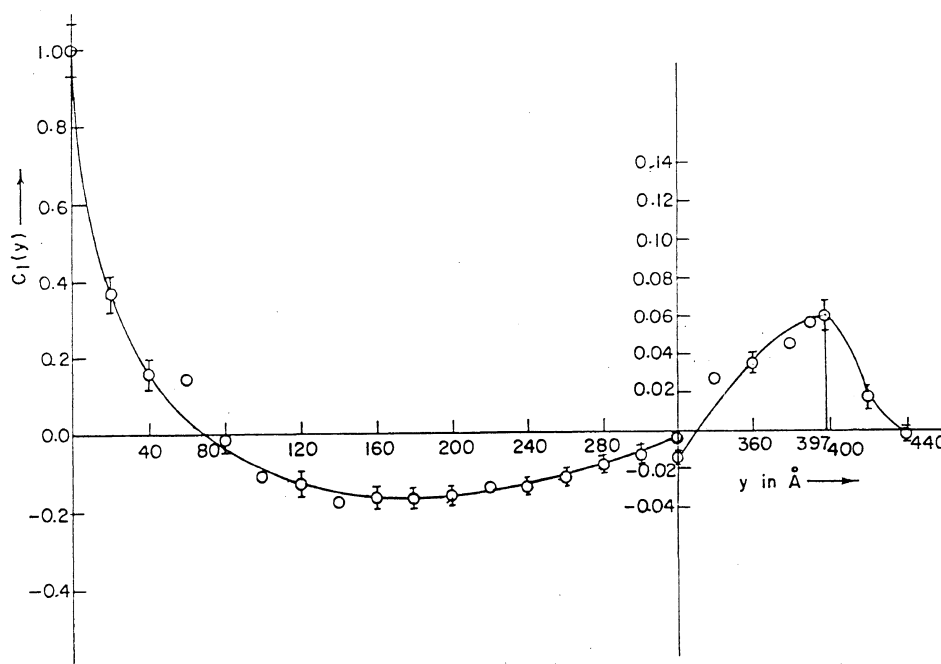


Figure 4. Curve of one-dimensional correlation function  $C_1(y)$  plotted against  $y$  with error bars.

'D' is noted on the curve. The 5% fluctuation in the intensity data in case of a sample produces no change in the position of the first subsidiary maximum as verified by the computation of  $C_1(y)$ .

The plot  $\tilde{I}(q) \cdot q$  versus  $q^{-2}$  of the sample is shown in Figure 5. The plot gives a straight line at the limiting region of the scattering curve. The value of standard deviation of intensities  $\sigma(\tilde{I})^{1/2}$  at the tail end of the SAXS pattern is 0.02 which is well within permissible limits. The coefficient of line of regression,  $\gamma$ , comes out to be 0.91 which is close to unity suggesting more or less the correctness of the data.

Other calculations were made applying the above theories and the results obtained are given below:

$$\begin{aligned} \bar{I}_1 &= (709.86 \pm 4.86) \text{ \AA} & \phi_{12} &= (0.095 \pm 0.002)\% \\ \bar{I}_2 &= (84.14 \pm 4.86) \text{ \AA} & \phi_1 &= (89.4 \pm 0.6)\% \end{aligned}$$

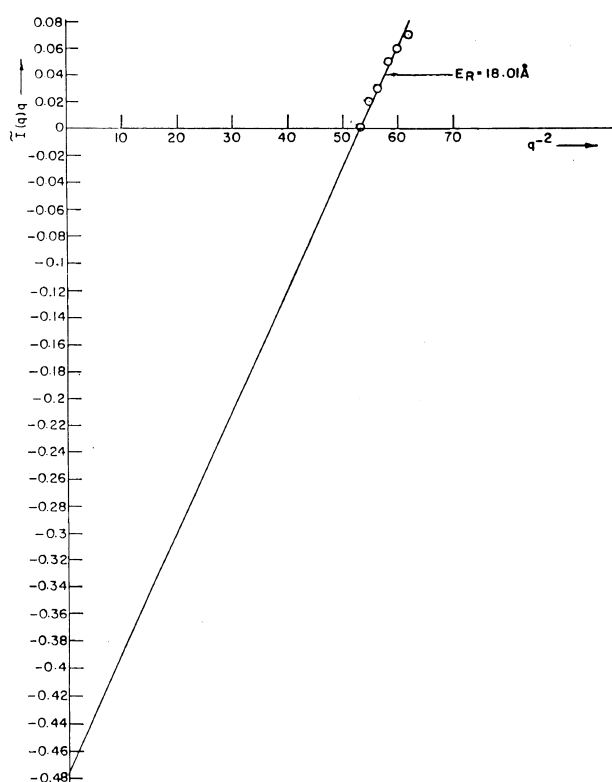


Figure 5. Ruland plot  $\tilde{I}(q) \cdot q$  versus  $q^{-2}$ .

$$\begin{aligned} \bar{I}_r &= (75.23 \pm 1.5) \text{ \AA} & \phi_2 &= (10.6 \pm 0.6)\% \\ \bar{I}_c &= (142 \pm 9.41) \text{ \AA} & R &= (2.78 \times 10^{-3} \pm 1.97 \times 10^{-4}) \text{ \AA}^{-2} \\ S/V &= (5.04 \times 10^{-3}) \text{ \AA}^{-1} & E_R &= (17.67 \pm 0.02) \text{ \AA} \\ D &= 397 \text{ \AA} & E_v &= (19.09 \pm 1.12) \text{ \AA} \\ 2E_v/D &= (10.77 \pm 0.79)\% \end{aligned}$$

The values obtained here are quite compatible with the internationally accepted values for various synthetic polymers and are given in Tables I and II.

## DISCUSSION AND CONCLUSION

As mentioned earlier for an ideal two-phase structure, the intercept of the Ruland plot vanishes leading to application of Porod's law. But when this intercept is negative, the system is considered to be a non-ideal two-phase system. In our case, the intercept in Figure 5 has a finite negative value which shows that PBLG comes under the non-ideal two-phase system.

For a dilute system,  $C(r)$  initially remains positive and comes to zero at large  $r$ .<sup>22</sup> But in case of a non-ideal two-phase system, it oscillates at large  $r$  as shown in Figure 2.

The values of standard deviation of intensities at the tail end of the SAXS pattern of the sample were found to be much less than 0.5 indicating the correctness of the data.<sup>23</sup> Also, the closeness of coefficient of line of regression to unity suggests more or less the statistical correctness of the data.<sup>24</sup>

The widths of transition layers  $E_v$  and  $E_R$  as determined by the two methods are approximately equal, which confirms the correctness of data collection and the method of analysis.

*Acknowledgment.* The author expresses deep gratitude to her guide, Prof. Dr. T. Misra, and her father, Prof. Dr. T. Ratho, an eminent Physicist, for helpful suggestions during the progress of this work.

## REFERENCES

1. G. Porod, *Kolloid Z.*, **124**, 83 (1951).
2. G. Porod, *Kolloid Z.*, **125**, 51 (1952).
3. E. Helfand, *Acc. Chem. Res.*, **8**, 259 (1975).
4. E. Helfand and V. Tagmi, *Polym. Lett.*, **9**, 741 (1971).
5. C. G. Vonk, *J. Appl. Cryst.*, **6**, 81 (1973).

Table I.

Sample	Authors	$(2E_v/D)/\%$
1 Poly( $\gamma$ -benzyl-L-glutamate) (DP 1100)	Rath	$(10.77 \pm 0.79)$
2 Short-chain branched polyethylene, stamylan 1500 (DSM) quenched from the melt	Vonk (1973)	17
3 Poly( $\gamma$ -benzyl-L-glutamate) (DP 1460)	Misra <i>et al.</i> (1993)	$(18.15 \pm 1.07)$
4 Polypropylene-carlona (shell) HM-61	Vonk (1973)	16

Table II.

Sample	Authors	$\bar{I}_c/\text{\AA}$
1 Poly( $\gamma$ -benzyl-L-glutamate) (DP 1100)	Rath	$(142 \pm 9.41)$
2 Gamma-irradiated (3 Mrad) methyl metha crystal grafted onto nylon 6 (grafting percentage 76%)	Misra <i>et al.</i> (1993)	$(317.9 \pm 6.2)$
3 Poly( $\gamma$ -benzyl-L-glutamate) (DP 1460)	Misra <i>et al.</i> (1993)	$(124.0 \pm 0.92)$

6. W. Ruland, *J. Appl. Cryst.*, **4**, 70 (1971).
7. E. Iizuka, *Adv. Polym. Sci.*, **20**, 79 (1976).
8. S. Sobajima, *J. Phys. Soc. Jpn.*, **23**, 1070 (1967).
9. G. T. Stewart, *Mol. Cryst. Liq. Cryst.*, **1**, 563 (1966).
10. O. Kratky, in "Small-Angle X-Ray Scattering," H. Brumberger, Ed., Gordon and Breach, New York, N.Y. (1967).
11. T. Misra, K. C. Patra, and T. Patel, *Colloid Polym. Sci.*, **262**, 611 (1984).
12. P. Debye, H. R. Anderson, and H. Brumberger, *J. Appl. Phys.*, **28**, 279 (1957).
13. J. Mering and D. Tchoubar, *J. Appl. Cryst.*, **1**, 153 (1965).
14. F. J. Balta Calleja and C. G. Vonk, "X-Ray Scattering of Synthetic Polymers," Elsevier Science Publishers, Amsterdam, 1989, p 264.
15. P. Mittelbach and G. Porod, *Kolloid Z.-Z. Polym.*, **202**, 40 (1965).
16. W. Ruland, *Colloid Polym. Sci.*, **255**, 417 (1977).
17. F. J. Balta Calleja and C. G. Vonk, "X-Ray Scattering of Synthetic Polymers," Elsevier Science Publisher, Amsterdam, 1989, p 242.
18. W. Ruland, *Prog. Coll. Polym. Sci.*, **57**, 192 (1975).
19. G. Kortleve, C. A. F. Tuijnman, and C. G. Vonk, *J. Polym. Sci., A2*, **10**, 123 (1972).
20. J. Rathje and W. Ruland, *Coll. Polym. Sci.*, **254**, 358 (1976).
21. C. G. Vonk, *J. Appl. Cryst.*, **8**, 340 (1975).
22. A. Guinier and G. Fournet, "Small-Angle Scattering of X-Rays," John Wiley & Sons, Inc., New York, N.Y. 1955, p 79.
23. C. G. Vonk, *J. Appl. Cryst.*, **4**, 340 (1971).
24. J. Topping, "Errors of Observation and Their Treatment," 4th ed, Chapman and Hall, London, 1972.